catalysts

MDPI

Article

A Promising Cobalt Catalyst for Hydrogen Production

Bogdan Ulejczyk [1,*], Paweł Jóźwik [2], Michał Młotek [1] and Krzysztof Krawczyk [1]

[1] Faculty of Chemistry, Warsaw University of Technology, Noakowskiego 3, 00-664 Warszawa, Poland; michal.mlotek@pw.edu.pl (M.M.); kraw@ch.edu.pl (K.K.)
[2] Faculty of Advanced Technologies and Chemistry, Military University of Technology, Gen. S. Kaliskiego 2, 00-908 Warszawa, Poland; pjozwik@wat.edu.pl
* Correspondence: bulejczyk@ch.pw.edu.pl

Abstract: In this work, a metal cobalt catalyst was synthesized, and its activity in the hydrogen production process was tested. The substrates were water and ethanol. Activity tests were conducted at a temperature range of 350–600 °C, water to ethanol molar ratio of 3 to 5, and a feed flow of 0.4 to 1.2 mol/h. The catalyst had a specific surface area of 1.75 m^2/g. The catalyst was most active at temperatures in the range of 500–600 °C. Under the most favorable conditions, the ethanol conversion was 97%, the hydrogen production efficiency was 4.9 mol (H_2)/mol(ethanol), and coke production was very low (16 mg/h). Apart from hydrogen and coke, CO_2, CH_4, CO, and traces of C_2H_2 and C_2H_4 were formed.

Keywords: hydrogen; ethanol; catalyst

check for updates

Citation: Ulejczyk, B.; Jóźwik, P.; Młotek, M.; Krawczyk, K. A Promising Cobalt Catalyst for Hydrogen Production. *Catalysts* **2022**, *12*, 278. https://doi.org/10.3390/catal12030278

Academic Editors: José Antonio Calles and Angelo Vaccari

Received: 2 February 2022
Accepted: 25 February 2022
Published: 1 March 2022

Publisher's Note: MDPI stays neutral with regard to jurisdictional claims in published maps and institutional affiliations.

1. Introduction

The global consumption of primary energy is increasing rapidly. From 2000 to 2019, primary energy consumption increased from 109,583 TWh to 162,194 TWh [1]. Such an increase in energy consumption causes increased fossil fuel consumption and CO_2 emissions, which increased by 11.32 billion tonnes. Renewable energy production is growing all the time, but too slowly to compensate for the increased energy demand. From 2000 to 2019, energy production from renewable sources increased from 2870 to 7017 TWh [1]. During this period, wind and solar energy were developed the most. Nowadays, hydrogen technologies are intensively researched. As hydrogen is not dependent on the weather, it may be a more stable energy source. It is thus necessary to develop effective technology for hydrogen production from the available renewable resources. Ethanol is a readily available raw material obtained from biomass. Ethanol production is perfectly controlled, and is a safe compound. The products of ethanol and water conversion should be hydrogen and carbon dioxide. These are produced in ethanol steam reforming (ESR) and water−gas shift reaction (WGSR). Unfortunately, many competing reactions are also possible. As a result, the post-reaction mixture may contain acetaldehyde, hydrocarbons, carbon monoxide, and coke. Our previous work showed the chemical mechanism in detail [2].

The aim of research on hydrogen production from ethanol and water is to minimize the formation of undesirable products. One of the research paths is the development of a selective and active catalyst. There are many different materials with catalytic properties when producing hydrogen from ethanol. Metals, e.g. cobalt, nickel, copper, and platinum, are often catalysts [3–8]. Of these, cobalt is very attractive because it is cheaper than noble metals. M. Konsolakis et al. [3] reported that cobalt catalysts achieved a higher ethanol conversion than nickel, copper, and iron catalysts. Additionally, cobalt catalysts are characterized by a lower coke production than nickel catalysts [9,10]. Various cobalt catalysts differing in the amount of cobalt, additives, support, or microstructure have been synthesized. Their stability, activity, and selectivity vary depending on the catalyst

structure. For example, M. Konsolakis et al. [3] reported that the optimal cobalt content is 20%. On the other hand, M. Greluk et al. [11] reported that the conversion of ethanol and the selectivity of ethanol conversion into hydrogen increased with increasing the cobalt content. The highest cobalt content was 30%, and this catalyst was the most active. The reason for these divergent conclusions of the two research groups could be the use of different catalyst support. H. Song et al. [12] compared the properties of cobalt catalysts (10 wt%) supported on three carriers, and reported that the carrier influenced the activity of the cobalt catalyst. Cobalt supported on zirconium oxide was the most active. However, using aluminum oxide as a support caused a lower catalyst activity. The least active was cobalt supported on titanium oxide. The activity of the catalysts was related to the cobalt dispersion (ratio of exposed cobalt atoms to total cobalt atoms). It was the largest on zirconium oxide and the smallest on titanium oxide. On the other hand, the specific surface did not matter, because, for zirconium oxide, it was six times smaller than aluminum oxide and two times smaller than titanium oxide.

Y. Li et al. [13] compared the effect of 16 additives (in the amount of 5%) on alumina-supported cobalt catalysts. The authors reported that the additives influenced the microstructure and activity of the catalyst in different ways. For example, calcium reduced the specific surface area of the catalyst the most, while sodium increased it the most. The size of the cobalt particles was decreased the most by scandium, but titanium increased it the most. These studies did not show a simple relationship between the microstructure and the activity of the catalyst. Na, K, Ni, Cu, Zn, Zr, Ce, La, and Fe increased the ethanol conversion, while Mg, Ca, Ti, Sc, V, Cr, and Mn decreased it. Copper accelerated the coking process the most, while sodium inhibited this process.

It is worth noting that the methodology of the catalyst synthesis is also crucial for the properties of the catalyst. Y. Liu et al. [14] reported that catalyst synthesis methods influenced its activity. The most active catalyst was synthesized by homogeneous precipitation using urea, enabling the highest specific surface area and the smallest cobalt particles. Ch. Wang et al. [15] reported that the addition of various surfactants to the metal precursor solution influenced the structure of the catalyst and its activity. Two surfactants were compared, polyvinylpyrrolidone (PVP) and cetyltrimethyl ammonium bromide (CTAB). Both chemical compounds increased the specific surface area of the catalyst and the porosity, with PVP causing a more significant surface development than CTAB. The specific surface area and porosity increased with increasing surfactant concentration. However, the same correlation between the surfactant concentration and the catalyst activity was not found. The use of CTAB at a lower concentration resulted in the most significant increase in ethanol conversion. On the other hand, for PVP, a greater increase in ethanol conversion was achieved with a lower PVP content. The influence of the catalyst synthesis method on its activity was not only observed for cobalt catalysts. E.V. Matus et al. [16] reported that the method of nickel catalyst synthesis also influenced their activity. Even the change in calcination temperature was significant as it changed the process yield. In addition, in other catalytic processes, the methodology of catalyst synthesis influences its activity, as reported by P. Vacharapong et al. [17].

Generally, despite testing a wide variety of materials, further work is needed to develop an effective and durable ethanol steam reforming catalyst. In this study, a pure metallic cobalt catalyst with no additives was used. The metal catalyst is mechanically resistant, does not crumble, and does not dust. Excellent mechanical properties facilitate all operations with the catalyst, e.g., loading, unloading, and regeneration. The possibility of regeneration is an important factor because the activity of catalysts decreases during operation [3,9,10,13,15–22]. The reason for the decreased activity may be coking [3,10,13,16–21], sintering [3,10,13,15,20], and migration of the active phase [9,22]. Sintered catalysts and catalysts from which the active phase migrated must be replaced. In contrast, coke-coated catalysts can be regenerated. The metal catalyst does not sinter, and metal migration does not change its content on the surface. The metallic cobalt catalyst can be regenerated at high temperatures, which allows the deposited coke to be oxidized rapidly. The metal has an

excellent thermal conductivity. Therefore, the temperature in a reactor is easy to control. In reactors with supported catalysts, there are differences between the set-point temperature and the temperature of the catalytic bed. V. Palma et al. [23] reported that these differences depend on the type of carrier and the size of the grains.

In this work, a metal catalyst with a high specific surface area was synthesized. As it was pure cobalt, metal migration did not change its concentration on the catalyst surface. The metal did not sinter, and the melting point of cobalt is much higher than the process temperature. A very good thermal conductivity of cobalt resulted in a very short reactor start-up time. The catalyst bed temperature stabilized within 12 min

2. Results and Discussion

2.1. Catalyst Characterization

The obtained metal catalyst had a specific surface area of 1.75 m^2/g determined by nitrogen adsorption isotherm analysis using the BET isotherm (Brunauer−Emmett−Teller). This method was presented in our earlier articles [2,24]. The catalyst topography was analyzed by scanning electron microscopy (SEM), and its elemental composition was analyzed by energy-dispersive X-ray spectroscopy (EDX). These methods were presented in our earlier article [24]. Figures 1–4 show the catalyst surface and the distribution of elements before and after 20 h of operation. Coke was deposited on the catalyst, as evidenced by the presence of carbon on the catalyst surface after use. Oxygen was also present in the used catalyst. Despite the long-term reduction, there was also oxygen on the surface of the fresh catalyst. However, a comparison of the signal intensities from individual elements shows that oxygen was evenly distributed over the surface of the fresh catalyst. On the contrary, the distribution of elements for the used catalyst indicates that oxygen was present in a greater amount on the surface where carbon was also present. E. L. Viljoen and E. van Steen [25] reported that cobalt is easily oxidized by water. The oxidation process starts at 300 °C. The process conditions for producing hydrogen from ethanol and water enable cobalt oxidation by water. On the other hand, the presence of hydrogen makes it possible to reduce the cobalt oxide. Therefore, it is difficult to conclude whether the correlation between the simultaneous presence of oxygen and carbon results from the facilitated deposition of coke on the cobalt oxide or the difficult access of hydrogen to the surface covered with coke. The carbon structures of the whisker structures, previously reported by G. Słowik et al. [22] and by our group for the plasma-catalytic process [24], were not observed.

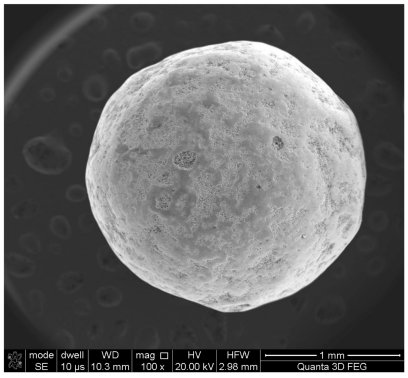

(**a**)

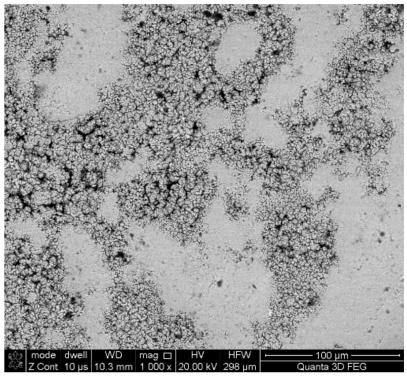

(**b**)

Figure 1. *Cont.*

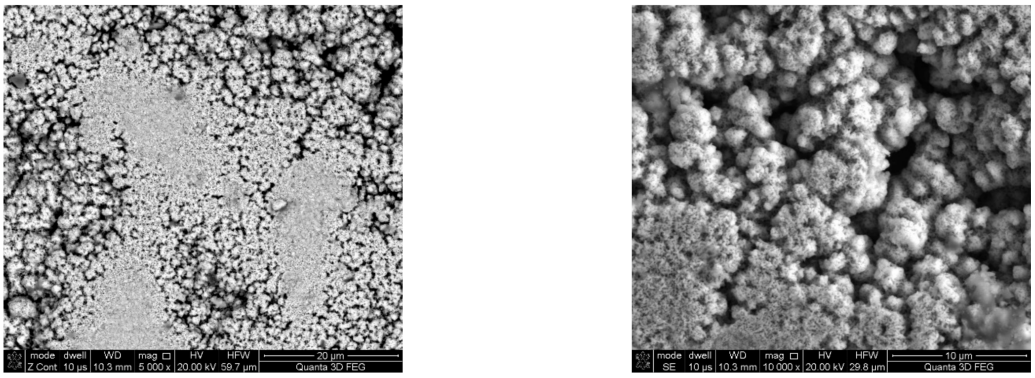

(**c**) (**d**)

Figure 1. SEM images of the fresh catalyst surface. (**a**) catalyst granule, (**b**) 1000-fold magnification, (**c**) 5000-fold magnification, (**d**) 10,000-fold magnification.

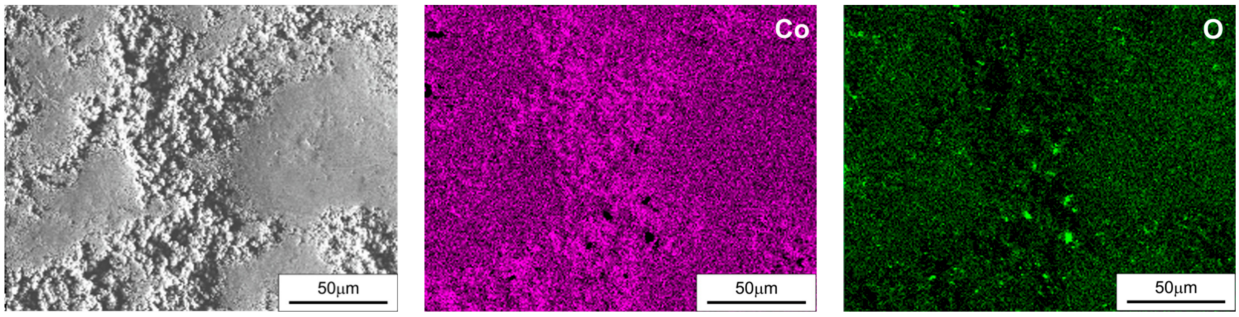

(**a**) (**b**) (**c**)

Figure 2. SEM image and EDX mapping analysis of the fresh catalyst. (**a**) SEM picture of the analyzed catalyst's surface, (**b**) distribution of cobalt, and (**c**) distribution of oxygen.

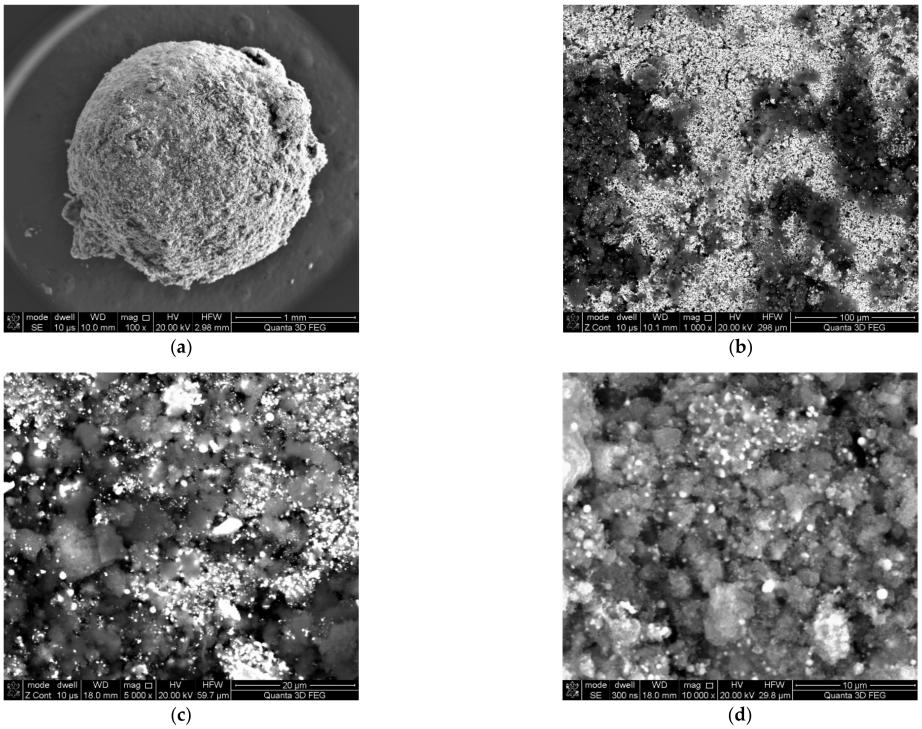

(**a**) (**b**)

(**c**) (**d**)

Figure 3. SEM images of the catalyst surface used. (**a**) catalyst granule, (**b**) 1000-fold magnification, (**c**) 5000-fold magnification, (**d**) 10,000-fold magnification.

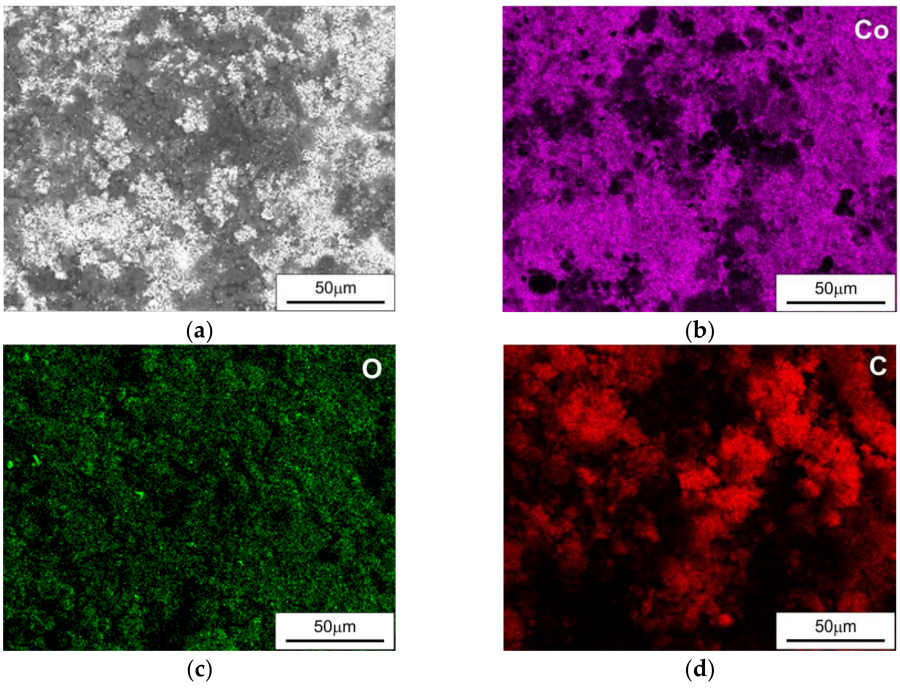

Figure 4. SEM images and EDX mapping analysis of the used catalyst. (**a**) SEM picture of the catalyst surface, (**b**) distribution of deposited cobalt, (**c**) distribution of oxygen, and (**d**) distribution of carbon.

2.2. Gaseous Products

The gaseous products were H_2, CO, CO_2, and CH_4 (Table 1). Moreover, C_2H_2 and C_2H_4 were present in minimal amounts (<0.1%). There was also water vapor (~2%) and ethanol in the cooled gas. The concentration of hydrogen was from 54 to 69%. The concentration of hydrogen increased with the increasing temperature. As the concentration of hydrogen increased, the concentration of CO_2 increased, and the concentrations of CO and CH_4 decreased.

Table 1. The concentration of gaseous products in gases after cooling and coke production.

Feed Flow Rate, mol/h		Temperature, °C	Concentration, %				Coke Production, g/h
Water	Ethanol		H_2	CO	CH_4	CO_2	
0.302	0.099	350	54.23	12.36	14.18	12.11	0.211
		400	57.21	10.64	11.21	13.47	0.260
		450	60.42	7.58	7.69	16.72	0.146
		500	64.24	6.91	4.32	16.8	0.256
		550	66.42	6.37	4.12	17.82	0.267
		600	66.11	7.42	4.01	16.8	0.288
0.601	0.199	350	53.82	14.25	15.34	9.24	0.571
		400	57.81	12.75	11.82	10.24	0.815
		450	60.02	9.51	8.21	14.75	0.418
		500	62.87	8.21	5.89	15.28	0.598
		550	64.38	6.82	5.15	16.2	0.740
		600	64.87	7.02	4.82	15.92	0.769

Table 1. *Cont.*

Feed Flow Rate, mol/h		Temperature, °C	Concentration, %				Coke Production, g/h
Water	Ethanol		H_2	CO	CH_4	CO_2	
0.901	0.301	350	61.08	14.68	12.05	5.27	1.333
		400	62.47	13.39	10.01	6.85	1.933
		450	64.54	8.52	6.91	12.46	1.560
		500	65.19	7.24	5.82	14.19	1.518
		550	65.42	7.03	5.44	14.28	1.780
		600	65.28	7.52	5.12	14.32	1.541
0.321	0.081	350	61.49	5.82	7.28	18.29	0.075
		400	61.78	5.21	6.92	18.72	0.089
		450	64.1	4.92	5.72	19.24	0.105
		500	67.25	4.42	3.3	19.65	0.145
		550	68.05	4.15	2.95	20.25	0.114
		600	68.01	4.26	3.08	19.98	0.146
0.333	0.066	350	62.49	5.21	6.24	18.61	0.083
		400	62.78	4.81	5.82	19.21	0.051
		450	64.82	4.01	4.53	20.31	0.018
		500	68.08	4.05	3.48	21.05	0.016
		550	68.92	3.82	2.94	21.31	0.016
		600	68.65	3.78	3.15	21.25	0.026

Apart from temperature, an important parameter influencing the concentration of CO, CO_2, and CH_4 was the molar ratio of water to ethanol. As the molar ratio of water to ethanol increased, the concentration of CO_2 increased. With a stoichiometric ratio of water to ethanol of 3, for the reaction (1):

$$C_2H_5OH + 3H_2O \leftrightarrows 6H_2 + 2CO_2 \quad (1)$$

only at a temperature of 450 °C and above was the concentration of CO_2 greater than the concentration of CO and CH_4. Increasing the water to ethanol molar ratio caused the concentration of CO_2, even at 350 °C, to be higher than the concentration of CO and CH_4.

CO and CH_4 are formed in the following reactions (reactions (2) and (3)) [26]:

$$C_2H_5OH + H_2O \leftrightarrows 4H_2 + CO \quad (2)$$

$$C_2H_5OH \leftrightarrows CH_4 + CO + H_2 \quad (3)$$

CO and CH_4 are undesirable products, and water promotes their further conversion [26,27]:

$$CH_4 + H_2O \leftrightarrows CO + 3H_2 \quad (4)$$

$$CO + H_2O \leftrightarrows H_2 + CO_2 \quad (5)$$

The use of water excess increases the production of H_2 and CO_2 and decreases the production of CO and CH_4.

2.3. Coke Formation

Coke production increases rapidly with increasing the feedstock flow (Table 1). The increase in coke production was greater than the increase in substrate flow. This indicates that coke was formed in large amounts and then consumed. The most likely sequence of reactions leading to the formation of coke was initiated by ethanol dehydration (reaction (6)) [26,28]:

$$C_2H_5OH \rightarrow C_2H_4 + H_2O \quad (6)$$

$$C_2H_4 \rightarrow C_2H_2 + H_2 \quad (7)$$

$$C_2H_2 \rightarrow 2C + H_2 \quad (8)$$

when coke was consumed in the hydration reaction (reaction (9)) [26]:

$$C + H_2O \leftrightarrows H_2 + CO \quad (9)$$

The high molar ratio of water to ethanol inhibited the ethanol dehydration reaction and accelerated the coke hydration reaction. Therefore, coke production decreased as the molar ratio of water to ethanol increased.

The coke production reached minimum values at high temperatures, ranging from 450 to 550 °C. Similarly, V. Palma et al. [19] reported that a low temperature promotes coking, whereas B. Banach et al. [29] reported that coke production peaked at temperatures in the range of 560–570 °C, and it depended on the type of carrier. The different results obtained on different catalysts indicate that the properties of the catalyst have a significant influence on the coking process.

2.4. Ethanol Conversion

The metal cobalt catalyst was active from 350 °C. The activity of the catalyst increased rapidly when the temperature increased up to 500 °C (Figures 5 and 6). The further increase in temperature had little effect on the ethanol conversion. Similar changes in the activity of various cobalt catalysts were observed by Y. Li et al. [13].

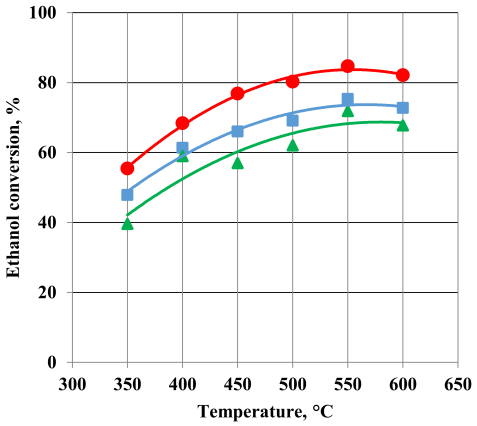

Figure 5. The influence of temperature and feed flow rate on ethanol conversion. Water to ethanol molar ratio in the feed = 3. Feed flow rate: ● = 0.4, ■ = 0.8, and ▲ = 1.2 mol/h.

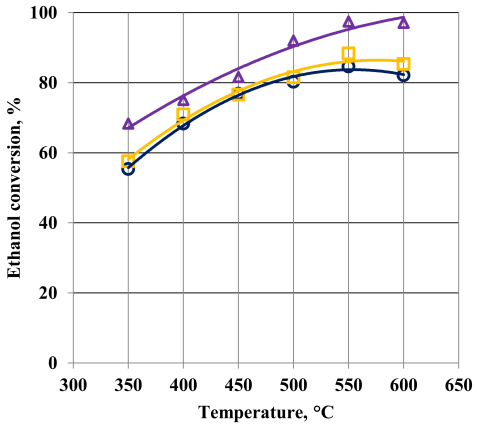

Figure 6. The influence of temperature and feed flow composition on ethanol conversion. Feed flow rate = 0.4 mol/h. Water to ethanol molar ratio in the feed: Δ = 5, □ = 4, and o = 3.

The ethanol conversion decreased with increasing the feed flow (Figure 5). This resulted from the shortening of the contact time of the reactants with the catalyst. An increase in the molar ratio of water to ethanol increased the ethanol conversion (Figure 6). Ethanol is more expensive than water, so it is worth using the excess water to obtain a higher ethanol conversion. Additional benefits of using excess water are reducing the production of coke, CH_4, and CO and increasing the production of H_2 and CO_2. On the other hand, the disadvantageous effect of using excessive water is the greater energy consumption necessary to heat and evaporate the water. Due to the energy cost in the industrial process of producing hydrogen from natural gas, the H_2O/C molar ratio is 2.5 [27], and efforts have been made to reduce it in new installations [30]. Q. Shen et al. [31] reported that the highest ethanol conversion was achieved with a water to ethanol molar ratio of 5 (H_2O/C molar ratio 2.5). The use of more water did not increase the ethanol conversion.

2.5. Hydrogen Yield

Figures 7 and 8 show the effect of temperature, feed flow rate, and feed stream composition on the hydrogen yield. The hydrogen yield increased with increasing the temperature, but already at 500 °C, it reached a high value. The increase in temperature to 600 °C had little effect on the hydrogen yield. The hydrogen yield decreased with increasing the feed flow rate. In contrast, the increase in the molar ratio of water to ethanol increased the hydrogen yield. The highest hydrogen production efficiency was 4.9 for high temperatures, the lowest flow, and the highest molar ratio of water to ethanol. Q. Shen et al. [31] also reported that the highest hydrogen yield was achieved at a high temperature and a high molar ratio of water to ethanol. The highest hydrogen yield was ~4.8 and was achieved for a higher molar ratio of water to ethanol compared to that used in this work.

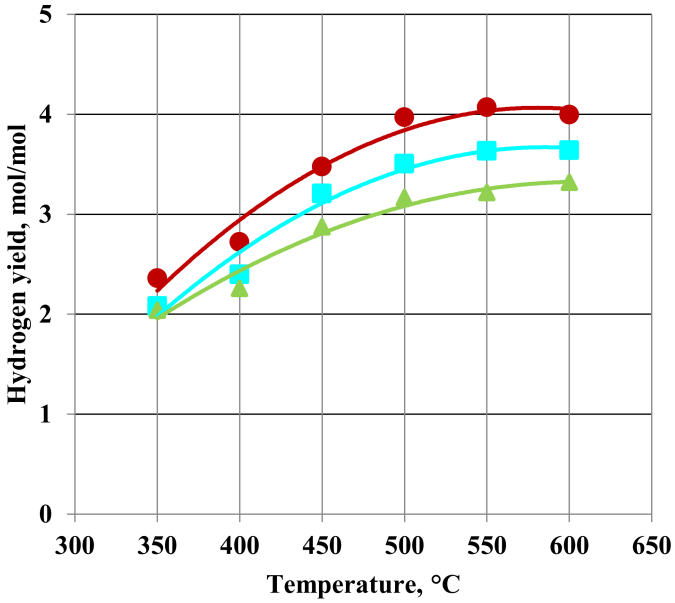

Figure 7. The influence of temperature and feed flow rate on hydrogen yield. Water to ethanol molar ratio in the feed = 3. Feed flow rate: ● = 0.4, ■ = 0.8, and ▲ = 1.2 mol/h.

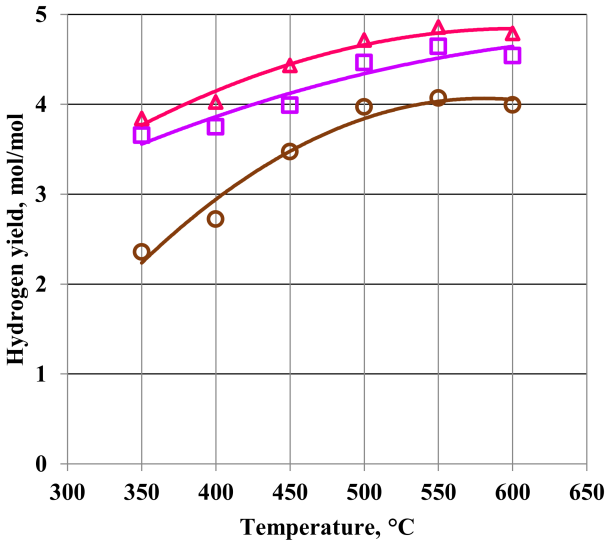

Figure 8. The influence of temperature and feed flow composition on the hydrogen yield. Feed flow rate = 0.4 mol/h. Water to ethanol molar ratio in the feed: Δ = 5, □ = 4, and o = 3.

3. Materials and Methods

3.1. Catalyst Preparation

The catalyst preparation scheme is shown in Figure 9. Firstly, powdered metallic cobalt was dissolved in nitric acid.

$$Co + 2HNO_3 \rightarrow Co(NO_3)_2 + H_2 \quad (10)$$

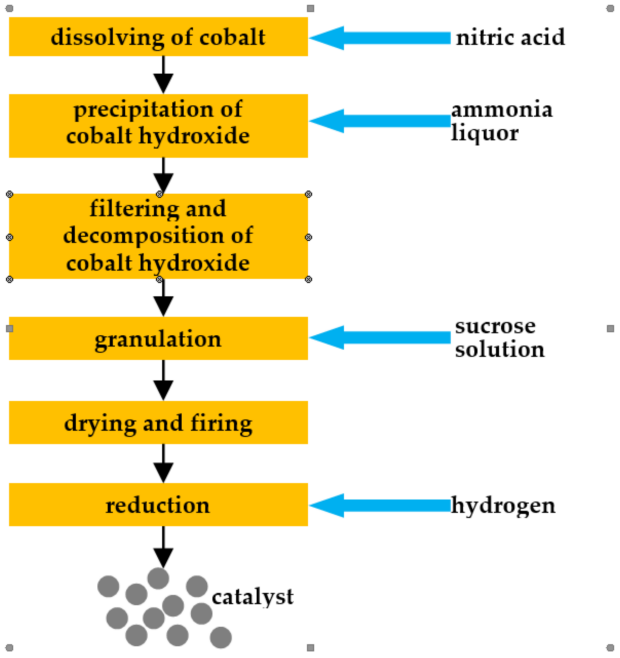

Figure 9. Schematic illustration of the cobalt catalyst preparation procedure.

Ammonia liquor was added to the obtained cobalt nitrate, and the cobalt hydroxide precipitated.

$$Co(NO_3)_2 + 2H_2O + 2NH_3 \rightarrow Co(OH)_2 + 2NH_4NO_3 \quad (11)$$

The obtained cobalt hydroxide was filtered and calcined at 600 °C for 5 h.

$$6Co(OH)_2 + O_2 \rightarrow 2Co_3O_4 + 6H_2O \quad (12)$$

The obtained cobalt oxide was wetly granulated in a disk granulator using a 20% sucrose solution as a granulating liquid. Next, the 0.8–2 mm fraction was separated on the sieves. The granules were dried for 24 h. Then, the granules were fired at 1250 °C for 5 h. After cooling down the granules, the 0.8–2 mm fraction was separated and reduced with hydrogen at a temperature of 300 °C for 6 h.

$$Co_3O_4 + 4H_2 \rightarrow 3Co + 4H_2O \quad (13)$$

3.2. Catalyst Activity Tests

The installation for conducting the catalyst activity tests is shown in Figure 10. A catalyst sample (2 g) was placed in a tubular quartz reactor with an internal diameter of 11 mm. After the substrates were introduced into the reactor, the heating started. The catalyst could not be preheated in the air as cobalt oxidizes at 80 °C. Catalyst activity tests were carried out at a temperature range of 350–600 °C. The temperature of 350 °C was the lowest temperature at which the catalyst showed activity. The maximum test temperature was set at 600 °C, as the energy cost of hydrogen production increased with increasing the temperature. Currently, research is being carried out on new solid oxide fuel cells (SOFCs) that may operate at temperatures up to 600 °C [32,33].

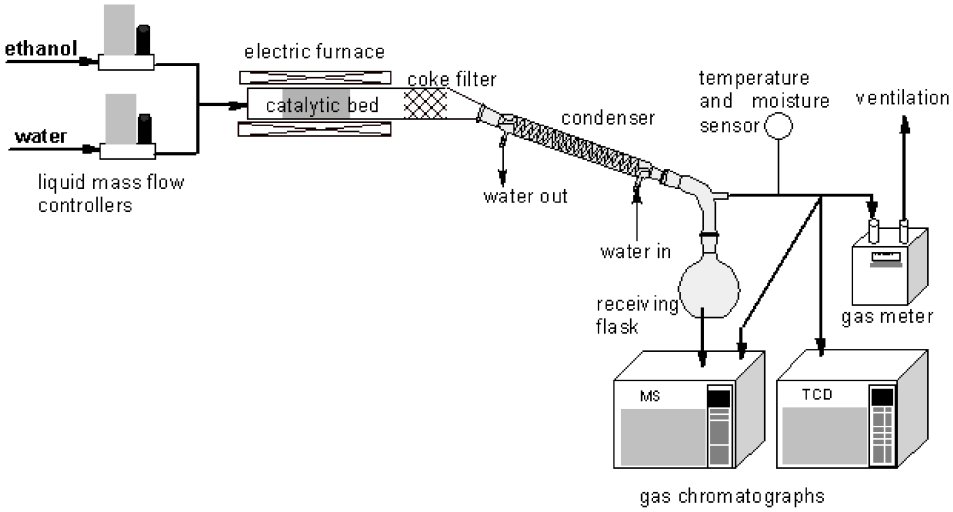

Figure 10. Scheme of the installation for the catalyst activity tests.

The molar ratio of water to ethanol ranged from 3 to 5. The molar feed flow rate ranged from 0.4 to 1.2 mol/h. The methods and apparatus used in the catalyst activity tests were described in detail in our previous works [2,24,34,35].

The ethanol conversion (X, %) and the hydrogen yield (Y, mol(H_2)/mol(C_2H_5OH)) were calculated from Formulas ((14) and (15)):

$$X = (F_{in}[C_2H_5OH] - F_{out}[C_2H_5OH])/F_{in}[C_2H_5OH]*100\%, \quad (14)$$

$$Y = F_{out}[H_2]/(F_{in}[C_2H_5OH - F_{out}[C_2H_5OH]), \quad (15)$$

$F_{in}[C_2H_5OH]$: ethanol feed flow, mol/h,
$F_{out}[C_2H_5OH]$: flow of the ethanol leaving the reactor, mol/h,
$F_{out}[H_2]$: hydrogen production rate, mol/h.

4. Conclusions

The cobalt catalyst is a promising catalyst for hydrogen production from a water and ethanol mixture. The metal catalyst is resistant to sintering and active phase migration. It enables high ethanol conversion and high hydrogen production efficiency. The conditions conducive to obtaining high conversion and yield values are high temperature, low feed flow, and excess of water. The highest ethanol conversion and hydrogen production efficiency were achieved for a temperature of 550 °C, substrate flow of 0.4 mol/h, and water to ethanol molar ratio of 5. Under these conditions, the coke production was low, at 16 mg/h. The use of water in excess was beneficial, as increasing the water to ethanol molar ratio increased the concentration of H_2 and CO_2. In contrast, the concentration of CH_4 and CO decreased. The high activity of the cobalt catalyst at a temperature of 500–600 °C means that it can be used in the production of hydrogen to supply solid oxide fuel cells operating at low temperatures.

Author Contributions: Conceptualization, B.U.; methodology, B.U., M.M. and P.J.; validation, B.U., K.K., P.J. and M.M.; formal analysis, B.U.; investigation, B.U. and P.J.; resources, B.U. and P.J.; data curation, B.U.; writing—original draft preparation, B.U.; writing—review and editing, B.U.; supervision, B.U.; funding acquisition, K.K. All authors have read and agreed to the published version of the manuscript.

Funding: This research was funded by the Warsaw University of Technology.

Data Availability Statement: Not applicable.

Conflicts of Interest: The authors declare no conflict of interest.

References

1. Ritchie, H.; Roser, M. Energy, Published Online at OurWorldInData.org. Available online: https://ourworldindata.org/energy (accessed on 1 February 2022).
2. Ulejczyk, B.; Nogal, Ł.; Młotek, M.; Falkowski, P.; Krawczyk, K. Hydrogen production from ethanol using a special multi-segment plasma-catalytic reactor. *J. Energy Inst.* **2021**, *95*, 179–186. [CrossRef]
3. Konsolakis, M.; Ioakimidis, Z.; Kraia, T.; Marnellos, G.E. Hydrogen Production by Ethanol Steam Reforming (ESR) over CeO_2 Supported Transition Metal (Fe, Co, Ni, Cu) Catalysts: Insight into the Structure-Activity Relationship. *Catalysts* **2016**, *6*, 39. [CrossRef]
4. Matus, E.; Sukhova, O.; Ismagilov, I.; Kerzhentsev, M.; Stonkus, O.; Ismagilov, Z. Hydrogen Production through Autothermal Reforming of Ethanol: Enhancement of Ni Catalyst Performance via Promotion. *Energies* **2021**, *14*, 5176. [CrossRef]
5. Rajabi, Z.; Jones, L.; Martinelli, M.; Qian, D.; Cronauer, D.C.; Kropf, A.J.; Watson, C.D.; Jacobs, G. Influence of Cs Promoter on Ethanol Steam-Reforming Selectivity of Pt/m-ZrO_2 Catalysts at Low Temperature. *Catalysts* **2021**, *11*, 1104. [CrossRef]
6. Hamryszak, Ł.; Kulawska, M.; Madej-Lachowska, M.; Śliwa, M.; Samson, K.; Ruggiero-Mikołajczyk, M. Copper Tricomponent Catalysts Application for Hydrogen Production from Ethanol. *Catalysts* **2021**, *11*, 575. [CrossRef]
7. Cifuentes, B.; Valero, M.F.; Conesa, J.A.; Cobo, M. Hydrogen Production by Steam Reforming of Ethanol on Rh-Pt Catalysts: Influence of CeO_2, ZrO_2, and La_2O_3 as Supports. *Catalysts* **2015**, *5*, 1872–1896. [CrossRef]
8. da Costa-Serra, J.F.; Navarro, M.T.; Rey, F.; Chica, A. Sustainable Production of Hydrogen by Steam Reforming of Ethanol Using Cobalt Supported on Nanoporous Zeolitic Material. *Nanomaterials* **2020**, *10*, 1934. [CrossRef]
9. Greluk, M.; Rotko, M.; Turczyniak-Surdacka, S. Enhanced catalytic performance of La_2O_3 promoted Co/CeO_2 and Ni/CeO_2 catalysts for effective hydrogen production by ethanol steam reforming. *Renew. Energy* **2020**, *155*, 378–395. [CrossRef]
10. Contreras, J.L.; Figueroa, A.; Zeifert, B.; Salmones, J.; Fuentes, G.A.; Vázquez, T.; Angeles, D.; Nuño, L. Production of hydrogen by ethanol steam reforming using Ni–Co-ex-hydrotalcite catalysts stabilized with tungsten oxides. *Int. J. Hydrogen Energy* **2021**, *46*, 6474–6493. [CrossRef]
11. Greluk, M.; Rotko, M.; Słowik, G.; Turczyniak-Surdacka, S. Hydrogen production by steam reforming of ethanol over Co/CeO_2 catalysts: Effect of cobalt content. *J. Energy Inst.* **2019**, *92*, 222–238. [CrossRef]
12. Song, H.; Zhang, L.; Watson, R.B.; Braden, D.; Ozkan, U.S. Investigation of bio-ethanol steam reforming over cobalt-based catalysts. *Catal. Today* **2007**, *129*, 346–354. [CrossRef]
13. Li, Y.; Zhang, Z.; Jia, P.; Dong, D.; Wang, Y.; Hu, S.; Xiang, J.; Liu, Q.; Hu, X. Ethanol steam reforming over cobalt catalysts: Effect of a range of additives on the catalytic behaviors. *J. Energy Inst.* **2020**, *93*, 165–184. [CrossRef]
14. Liu, Y.; Murata, K.; Inaba, M. Steam Reforming of Bio-Ethanol to Produce Hydrogen over Co/CeO_2 Catalysts Derived from $Ce_{1-x}Co_xO_{2-y}$ Precursors. *Catalysts* **2016**, *6*, 26. [CrossRef]

15. Wang, C.; Wang, Y.; Chen, M.; Hu, J.; Yang, Z.; Zhang, H.; Wang, J.; Liu, S. Hydrogen production from ethanol steam reforming over Co–Ce/sepiolite catalysts prepared by a surfactant assisted coprecipitation method. *Int. J. Hydrogen Energy* **2019**, *44*, 26888–26904. [CrossRef]
16. Matus, E.V.; Okhlopkova, L.B.; Sukhova, O.B.; Ismagilov, I.Z.; Kerzhentsev, M.A.; Ismagilov, Z.R. Effects of preparation mode and doping on the genesis and properties of Ni/$Ce_{1-x}M_xO_y$ nanocrystallites (M = Gd, La, Mg) for catalytic applications. *J. F Nanopart. Res.* **2019**, *21*, 11. [CrossRef]
17. Vacharapong, P.; Arayawate, S.; Katanyutanon, S.; Toochinda, P.; Lawtrakul, L.; Charojrochkul, S. Enhancement of Ni Catalyst Using CeO_2–Al_2O_3 Support Prepared with Magnetic Inducement for ESR. *Catalysts* **2020**, *10*, 1357. [CrossRef]
18. Chen, Y.-J.; Huang, S.-H.; Uan, J.-Y.; Lin, H.-T. Synthesis of Catalytic Ni/Cu Nanoparticles from Simulated Wastewater on Li–Al Mixed Metal Oxides for a Two-Stage Catalytic Process in Ethanol Steam Reforming: Catalytic Performance and Coke Properties. *Catalysts* **2021**, *11*, 1124. [CrossRef]
19. Palma, V.; Ruocco, C.; Meloni, E.; Ricca, A. Influence of Catalytic Formulation and Operative Conditions on Coke Deposition over CeO_2-SiO_2 Based Catalysts for Ethanol Reforming. *Energies* **2017**, *10*, 1030. [CrossRef]
20. Mhadmhan, S.; Natewong, P.; Prasongthum, N.; Samart, C.; Reubroycharoen, P. Investigation of Ni/SiO_2 Fiber Catalysts Prepared by Different Methods on Hydrogen production from Ethanol Steam Reforming. *Catalysts* **2018**, *8*, 319. [CrossRef]
21. Palma, V.; Ruocco, C.; Meloni, E.; Gallucci, F.; Ricca, A. Enhancing Pt-Ni/CeO_2 performances for ethanol reforming by catalyst supporting on high surface silica. *Catal. Today* **2018**, *307*, 175–188. [CrossRef]
22. Słowik, G.; Greluk, N.; Rotko, M.; Machocki, A. Evolution of the structure of unpromoted and potassium-promoted ceriasupported nickel catalysts in the steam reforming of ethanol. *Appl. Catal. B Environ.* **2018**, *221*, 490–509. [CrossRef]
23. Palma, V.; Ruocco, C.; Castaldo, F.; Ricca, A.; Boettge, D. Ethanol steam reforming over bimetallic coated ceramic foams: Effect of reactor configuration and catalytic support. *Int. J. Hydrogen Energy* **2015**, *37*, 12650–12662. [CrossRef]
24. Ulejczyk, B.; Nogal, Ł.; Jóźwik, P.; Młotek, M.; Krawczyk, K. Plasma-Catalytic Process of Hydrogen Production from Mixture of Methanol and Water. *Catalysts* **2021**, *11*, 864. [CrossRef]
25. Viljoen, E.L.; van Steen, E. Rate of Oxidation of a Cobalt Catalyst in Water and Water/Hydrogen Mixtures: Influence of Platinum as a Reduction Promoter. *Catal. Lett.* **2009**, *133*, 8–13. [CrossRef]
26. de Souza, G.; Balzaretti, N.M.; Marcílio, N.R.; Perez-Lopez, O.W. Decomposition of Ethanol Over Ni-Al Catalysts: Effect of Copper Addition. *Procedia Eng.* **2012**, *42*, 335–345. [CrossRef]
27. Rostrup-Nielsen, J.R. Catalytic Steam Reforming. In *Catalysis Science and Technology*; Anderson, J.R., Boudart, M., Eds.; Springer-Verlag: Berlin/Heidelberg, Germany, 1984; Volume 5, pp. 3–117. [CrossRef]
28. Rye, R.R.; Hansen, R.S. Flash Decomposition of Acetylene, Ethylene, Ethane, and Methane on Tungsten. *J. Chem. Phys.* **1969**, *50*, 3585–3595. [CrossRef]
29. Banach, B.; Machocki, A.; Rybak, P.; Denis, A.; Grzegorczyk, W.; Gac, W. Selective production of hydrogen by steam reforming of bio-ethanol. *Catal. Today* **2011**, *176*, 28–35. [CrossRef]
30. Eyalarasan, K.; Tesfamariam, M.D.; Meleake, H.; Gebreyonas, A. Design of Process Plant for Producing Hydrogen from Steam Reforming of Natural Gas. *Int. J. Eng. Res. Technol.* **2013**, *2*, 746–754.
31. Shen, Q.; Jiang, Y.; Li, S.; Yang, G.; Zhang, H.; Zhang, Z.; Pan, X. Hydrogen production by ethanol steam reforming over Ni-doped $LaNi_xCo_{1-x}O_{3-\delta}$ perovskites prepared by EDTA-citric acid sol–gel method. *J. Sol-Gel Sci. Technol.* **2021**, *99*, 420–429. [CrossRef]
32. Thieu, C.A.; Yang, S.; Ji, H.I.; Kim, H.; Yoon, K.J.; Lee, J.H.; Son, J.W. Effect of secondary metal catalysts on butane internal steam reforming operation of thin-film solid oxide fuel cells at 500–600 °C. *Appl. Catal. B Environ.* **2020**, *263*, 118349. [CrossRef]
33. Fallah Vostakola, M.; Amini Horri, B. Progress in Material Development for Low-Temperature Solid Oxide Fuel Cells: A Review. *Energies* **2021**, *14*, 1280. [CrossRef]
34. Ulejczyk, B.; Nogal, Ł.; Młotek, M.; Krawczyk, K. Hydrogen production from ethanol using dielectric barrier discharge. *Energy* **2019**, *174*, 261–268. [CrossRef]
35. Ulejczyk, B.; Nogal, Ł.; Młotek, M.; Krawczyk, K. Enhanced production of hydrogen from methanol using spark discharge generated in a small portable reactor. *Energy Rep.* **2022**, *8*, 183–191. [CrossRef]